Proceedings of the ASME 2010 3rd Joint US-European Fluids Engineering Summer Meeting and 8th International Conference on Nanochannels, Microchannels, and Minichannels
FEDSM-ICNMM2010
August 1-5, 2010, Montreal, Canada

FEDSM-ICNMM2010-30605

MICRO-PIV AND CFD STUDIES SHOW NON-UNIFORM WALL SHEAR STRESS DISTRIBUTIONS OVER ENDOTHELIAL CELLS

Sharul S. Dol
Department of Mechanical and Manufacturing Engineering University of Calgary
Calgary, Alberta, Canada
ssbdol@ucalgary.ca

M. Mehdi Salek
Department of Mechanical and Manufacturing Engineering University of Calgary
Calgary, Alberta, Canada
msalek@ucalgary.ca

Kayla D. Viegas
Department of Mechanical and Manufacturing Engineering
University of Calgary
Calgary, Alberta, Canada
kdviegas@ucalgary.ca

Kristina D. Rinker
Centre for Bioengineering Research and Education,
Department of Chemical and Petroleum Engineering,
Department of Physiology and Biophysics
University of Calgary
Calgary, Alberta, Canada
tina.rinker@ucalgary.ca

Robert J. Martinuzzi
Department of Mechanical and Manufacturing Engineering
University of Calgary
Calgary, Alberta, Canada
rmartinu@ucalgary.ca

ABSTRACT

Wall shear stress acting on arterial walls is an important hemodynamic force determining vessel health. A parallel-plate flow chamber with a 127 μm-thick flow channel is used as an *in vitro* system to study the fluid mechanics environment. It is essential to know how well this flow chamber performs in emulating physiologic flow regimes especially when cultured cells are present. Hence, the objectives of this work are to computationally and experimentally study the characteristic of the flow chamber in providing a defined flow regime and shear stress to cultured cells and to map wall shear stress distributions in the presence of an endothelial cell layer. Experiments and modeling were performed for the nominal wall shear stresses of 2 and 10 dyn/cm^2. Without endothelial cells, the flow field is uniform over 95% of the chamber cross-section and the surfaces are exposed to the target stress level. Using PIV velocity data, the endothelial cell surfaces were re-constructed and flow over these surfaces was then simulated via FLUENT. Once endothelial cells are introduced, local shear variations are large and the velocity profiles are no longer uniform. Due to the velocity distribution between peaks and valleys, the local wall shear stresses range between 47-164% of the nominal values. This study demonstrates the non-uniform shear stress distribution over the cells is non-negligible especially in small vessels or where blockage is important.

Keywords: Endothelial cells, Parallel-plate flow chamber

INTRODUCTION

The endothelium consists of a monolayer of vascular endothelial cells and lines the internal surface of the highly dynamic blood vessels. Since the vascular endothelium forms an interface between the blood and the underlying layers of the vessel walls, it is constantly exposed to flow-induced shear stresses. Indeed, endothelial cells are able to detect changes in mechanical forces and subsequently trigger a variety of responses that affect their structure and functions. For example, regions of altered shear stress and disturbed flow have been linked to the formation of atherosclerotic plaques [1, 2, 3]. This accumulation results in a narrowed vessel lumen and hardening of the arteries; each of these factors eventually affects blood flow and can lead to vascular disease and bacterial infection. Once circulating bacteria have invaded the endothelium, they can easily progress deeper and spread throughout the tissues. High shear stress ($\geq$10 dyn/cm^2), which generally occurs through straight portions of the arteries, corresponds to healthy, protective regions, while low shear stress ($\leq$4 dyn/cm^2), which is often found at arterial branch points and areas of curvature, results in areas highly susceptible to pathogens and disease and is difficult to treat with conventional therapies [4].

Even though the effects of shear stress on vascular endothelial cells have been investigated extensively, many difficulties arise in studying the *in vivo* responses of the endothelium to shear stress due to the complex structure of the blood vessels and lack of resolved measurements with current

technologies [5, 6]. To overcome such limitations of *in vivo* approaches as well as to study the dynamic response of vascular endothelial cells to controlled levels of fluid shear stress, various types of *in vitro* systems that allow cultured endothelial cells to be exposed to well-defined flow conditions have been developed. These systems include orbital shakers [7], cone and plate viscometers, and parallel-plate flow chambers (PPFC) [8, 9, 10]. Among *in vitro* systems employed to study the effects of flow conditions on endothelial cells, PPFC have been the most commonly used to achieve a fully developed laminar flow within the channel of the chamber. A PPFC sets two plates in parallel to constitute a thin rectangular flow channel in between which a monolayer of cells is seeded on either side. The simplicity of the concept has contributed to its usage in many different applications of biomedical research (*e.g*. platelet adhesion, cell morphology, and cell responses to applied shear stress).

These conventional PPFC, however, have shown weaknesses and problems. In these chambers, flow should be steady and uniform over the length and span of the plate. Therefore, it is assumed that cells in the chamber are exposed to the same conditions regardless of their location. Under such conditions, responses from the endothelial cell monolayer can be determined by pooling cells from the whole chamber; therefore, results from these studies reflect an average cell response over the entire plate**.** However, Anderson et *al*. [9] found that flow regimes in commercially available perfusion chambers are not constant and shear stresses that are imparted to cells are location dependent at the cellular level. Furthermore, these flow fields differ between chambers as well according to their geometry and set flow rate. Hence, cells on one side of a chamber may experience a different stress than those on the opposite side. This complicates the comparisons of outcome measures if different chambers were used, even if target stress regimes are comparable.

This flow field non-uniformity is not always due to chamber design differences. When dealing with dimensions on the order of microns to hundreds of microns, standard machining tolerances can also cause non-negligible variations in the chamber height and local shear stresses. McCann et *al*. [10] found that even in a custom-built parallel plate flow chamber that was machined and assembled using well established protocols, the average velocity and the corresponding average channel height were non-uniform over the plate area. The shear stress values deviated from the average shear stress by as much as 11% across the channel area. Their chamber cross section thickness and Particle image velocimetry (PIV) uncertainty associated with the shear stress data was 330 μm and ±0.01 dyn/cm^2 respectively. Sensitive cell responses, such as that involving cell signalling and gene expression, may not be consistent over the chamber area in the environment of these non-uniform flows [11].

Knowing the actual subcellular force distribution on endothelial cells due to blood flow is important to understand the role of mechanical loading on the vascular endothelium. Simple explanations (*e.g.* low shear stress triggers atherosclerosis) have eluded researchers, and there is a growing recognition that other factors or unique combinations of factors are important determinants of endothelial dysfunction [11].

Much of the research to date on endothelial cells response to flow has failed to consider the entire hemodynamic environment. This is probably due, in large part, to the inability to measure flow over endothelial cells at the subcellular level. Researchers have relied heavily on computational fluid dynamics (CFD) methodologies without measuring the actual flows over cells [12]. Flow computations have been performed either with actual cell surface topography obtained from microscopy [13, 14] or by sinusoidal models [15]. Both methods gave similar spatial characteristics (*e.g.* shear stress distributions) but their magnitudes greatly differ. Barbee [11] found that simulation of flow over the real endothelial surface geometry revealed qualitative and quantitative differences compared to the sinusoidal model. To the authors' knowledge, none of these results are validated experimentally. The complexity of the flow pattern due to the cell height variations especially in micro-scale chambers needs to be examined with some degree of certainty.

PIV combines the accuracy of the quantitative velocity information of laser Doppler velocimetry with the global flow imaging capability of flow visualization. It also has the advantage of being able to measure fluid or particulate velocity vectors at many points in a flow field simultaneously. This makes the system suitable for resolving velocity information and associated properties over an extended region of the flow. In recent years, PIV techniques have been extended to the microscale, proving highly useful for acquiring flow data in microfluidic studies [16]. For example, PIV was used recently to obtain quantitative flow data in an *in vitro* model that mimics the flow conditions in microcapillaries [9, 10, 12].

Hence, the objectives of this study are; firstly, to evaluate performance of our micro-flow chamber, with a flow channel made by a 127 μm-thick silicon rubber gasket, in providing a defined flow regime and shear stress to cultured cells; secondly, to provide experimental results by the means of micro-particle image velocimetry in mapping the flow field over the endothelial cells. The results will be compared to our computational fluid dynamics modeling**.** No previous study has been performed at this micro-size level, therefore the overall objective of this study is to determine if the non-uniform shear stress distribution over the cells is non-negligible in very small channels (*e.g*. coronary microvessels).

NOMENCLATURE

d_p	Particle diameter
h	Height of the channel
n	Refractive index of fluid
Q	Volumetric flow rate
u	Stream-wise velocity
U_0	Average bulk velocity
w	Width of the channel
δz	Measurement depth
λ_0	Light wavelength

μ	Dynamic viscosity
θ	Light collection angle
τ_w	Wall shear stress

MATERIALS AND METHODS

Human umbilical vein endothelial cells (HUVEC) were cultivated in Endothelial Growth Media (EGM) at 37°C in a humidified incubator with 5% CO_2 through passage nine in tissue culture flasks using standard trypsin/EDTA enzymatic cell dissociation. HUVEC were stored long-term in liquid nitrogen in media containing 10% FBS and 10% DMSO. Cells for flow assays were prepared by seeding HUVEC on sterile glass microscope slides pretreated with 0.1% gelatin for 30 min in a sterile biosafety cabinet. HUVEC seeded on slides were maintained at 37°C and typically confluent in 2-4 days.

The flow chamber, shown in Fig. 1*a*, comprises a polycarbonate top plate with ports for inlet and outlet, a 127 μm-thick silicon rubber gasket with a removed rectangular section in the centre to form the flow channel (48 mm length x 12.5 mm width), a glass microscope slide with a confluent monolayer of HUVEC, and a second slide to help evenly distribute pressure applied by three C-clamps. Flow is obtained a constant-speed syringe pump. The nominal wall shear stress is obtained according to:

$$\tau_w = \frac{6Q\mu}{wh^2}$$

where Q is the volumetric flow rate, μ is the dynamic viscosity of water, w is the channel width, and h is the channel height.

PIV Measurements

Flow field information was obtained with the micro-PIV system (TSI) shown in Fig. 1*b*. Points 1-11 in Fig. 1*c* are the measurement locations in the chamber as given in Table 1. Duke red fluorescent particles (2.0 μm nominal diameter), for which the excitation maximum is 542 nm and the emission maximum is 612 nm were used as tracers (concentration of 0.3% by volume). The particles were excited with a 532 nm Nd:YAG laser (absorption efficiency better than the 90% of peak). A Nikon Plan Fluor 10X 0.3 NA objective lens was used with an inverted Nikon microscope. The images were captured by a CCD camera (POWERVIEW 4M with 2048 x 2048 pixels, pixel size is 7.4 μm) with a projection lens of 2X. This field of view is 0.76 x 0.76 mm^2 and each pixel images a 0.37 μm^2 area.

A volume illumination technique, as described by Meinhart et *al*. [17], was used to obtain PIV data at rates of 7.5Hz. The PIV measurement depth, δz, is related to the depth of focus of the recording lens and can be estimated by considering the effects of diffraction, geometrical optics and particle size:

$$\delta z = \frac{3n\lambda_0}{NA^2} + \frac{2.16d_p}{tan\theta} + d_p$$

where n is the refractive index of the fluid between the micro-fluidic device and the objective lens, λ_0 is the wavelength of light in a vacuum being imaged by the optical system, *NA* is the numerical aperture of the objective lens, θ is the light collection angle and d_p is the particle diameter. This results in a measurement depth uncertainty of 22.67 μm.

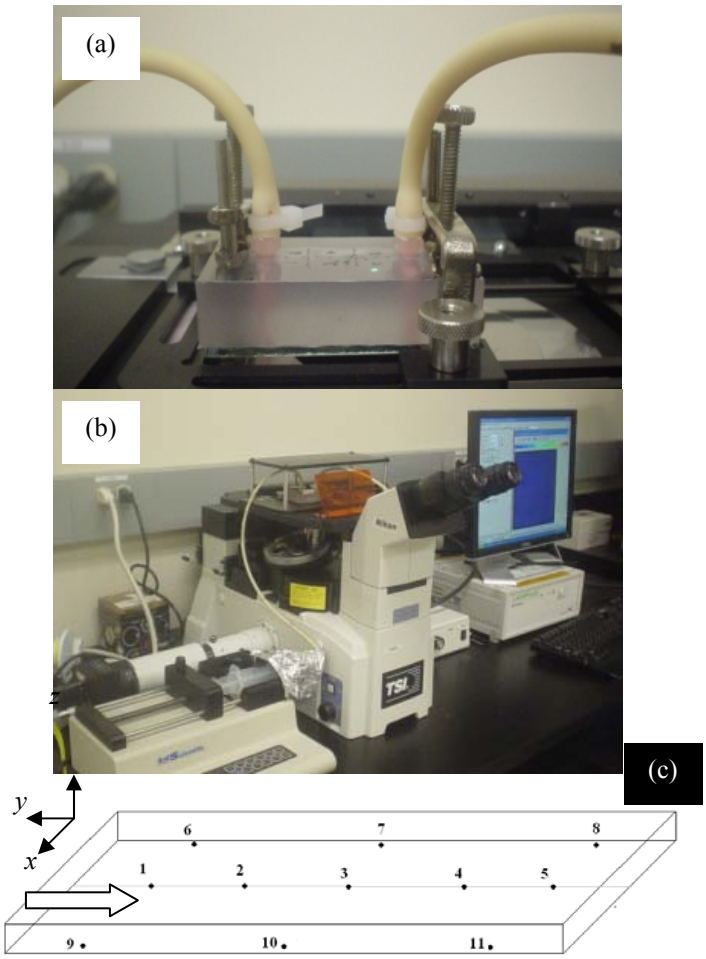

Figure 1 Experimental Set-up; (a) Flow Chamber; (b) Micro-PIV System; (c) Measurement Locations.

Point	*x* (mm)	*y* (mm)
1	6.25	39
2	6.25	31
3	6.25	23
4	6.25	15
5	6.25	7
6	1.00	39
7	1.00	23
8	1.00	7
9	11.50	39
10	11.50	23
11	11.50	7

Table 1 The Coordinates of the Measurement Locations.

Since only cases of steady state flow were considered, the signal to noise ratio was greatly improved by ensemble

averaging the correlation function across all frame pairs. An ensemble average of 100 image pairs was used for velocity estimation per acquisition. The TSI Insight® software was used to analyze the captured images using the cross-correlation technique. The spatial resolution, using 64 x 64 pixel interrogation spots, was 11.84 μm/spot. The level of background noise was low because the chamber was very thin, enabling use of higher particle concentrations and finer interrogation spots. An overlap of 50% of the interrogation area was used together with a Gaussian window function to minimize the loss of pairs. The time delay between image pairs ranged between 300 and 500 μs in all the experiments.

Experiments were performed at flow rates of 0.414 and 2.070 ml/min, for nominal wall shear stresses, τ_w of 2 and 10 dyn/cm^2 respectively in clean flow cell. The actual τ_w was determined from velocity gradient at the surface:

$$\tau_w = \mu \frac{du}{dz}\Big|_{wall}$$

where u is the velocity of the fluid along the boundary and z is the distance from the boundary. Velocity measurements were made 8 to 10 planes from the top wall to a plane nominally on the endothelial cell surface. Statistically, more than four million PIV data points were used to estimate a velocity profile plot.

The channel height without endothelial cells was confirmed to be ~127 μm at each of the PIV measurement locations by measuring the distance between particles adhering to each of the chamber walls. This was accomplished by focusing the microscope on particles adhering to one wall, and then traversing the microscope stage (with a 1-μm resolution) until particles on the opposite wall were in focus. In the presence of endothelial cells, velocity profile data were used to determine cells thickness by subtracting the original channel height with the new region of zero velocities, assumed to be within the cells boundaries.

CFD Modeling

The geometry and grids of two cases (flow cell with and without endothelial cells) were generated in Gambit and then exported to FLUENT version 6.3.2 to solve the flow. For the second case, the endothelial cell surfaces were reconstructed in Gambit using elevations measured from PIV at 225 points in a plane of 700 μm × 700 μm. The surface was interpolated to force the surface to pass through all vertices. The created surface is shown in the Fig. 2. The pure hexagonal grids with low skewness (<0.4) were generated in the domain. To determine the optimum number of grids, the average wall shear stress over the wavy surface of the cells was compared over a range of different number of cells. This comparison is summarized in Table 2 and shows an optimum number of grids of 98000 (less than 0.2% changes in wall shear stress by increasing the grids to 300000).

The flow in the clean flow cell and also over the re-constructed endothelial cell surfaces was then simulated via FLUENT. Continuity and steady Navier-Stokes equations were solved in three dimensions. Water as a medium with constant properties at 20°C was selected. For the clean flow cell, a uniform velocity profile, calculated based on the experimental flow rate, was imposed at the inlet and a no slip boundary condition was applied at the walls. For the second case (flow with endothelial cells), the inlet velocity profile, which was measured experimentally to account for the upstream presence of endothelial cells, was used. No slip boundary conditions were applied at the lateral walls and endothelial cell surfaces respectively. The results for micro-PIV and CFD were compared for velocity distribution and profiles as well as wall shear stress magnitudes.

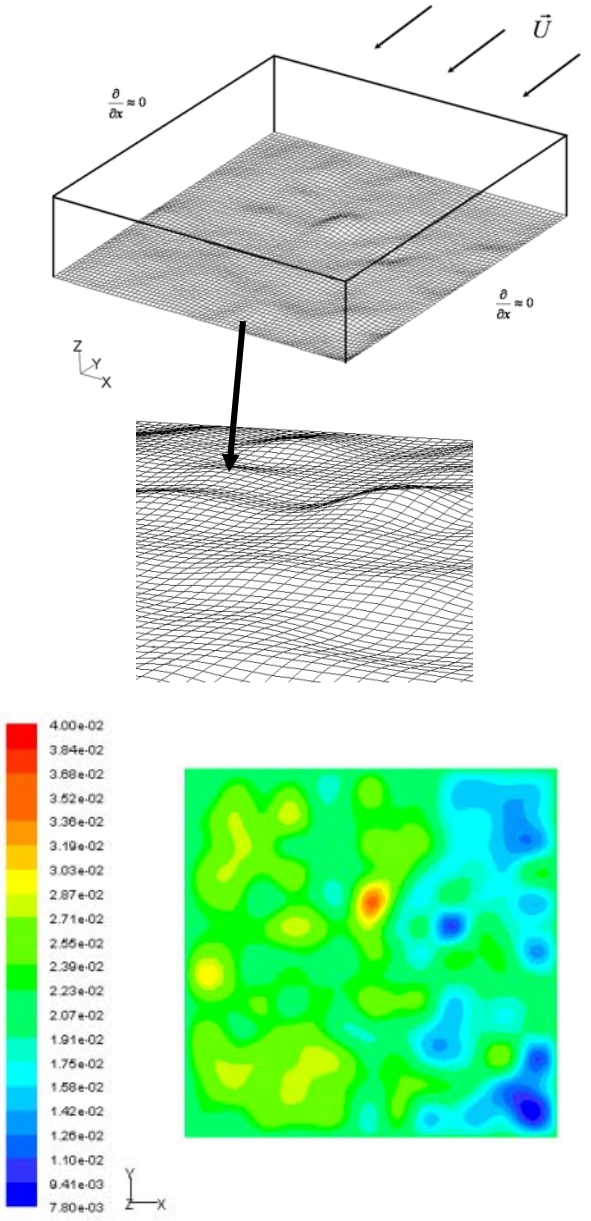

Figure 2 The Created Surface Presents a Wavy Shape (The Contour Colors Show Cell Thickness in mm unit).

Number of grids	98000	160000	300000
Average shear stress (Pa)	0.39008617	0.39054078	0.3907465

Table 2 Grid Independency Check.

RESULTS AND DISCUSSION

Without Endothelial Cells

In order to use a parallel plate flow chamber as a test case for further studies, it is essential to know how close the imparted stresses actually match the target (nominal) stresses. Without endothelial cells, the flow field is uniform over 95% of the chamber cross-section. Experiments confirmed that stress levels matched target levels within experimental uncertainty (2±3% and 10±6% for 2 and 10 dyn/cm^2 target stresses, respectively). Figure 3 shows the laminar parabolic velocity profiles obtained across the thickness of the flow chamber for Q = 0.414 ml/min. The experimental results agree well with the predicted CFD results, indicating PIV resolution is high.

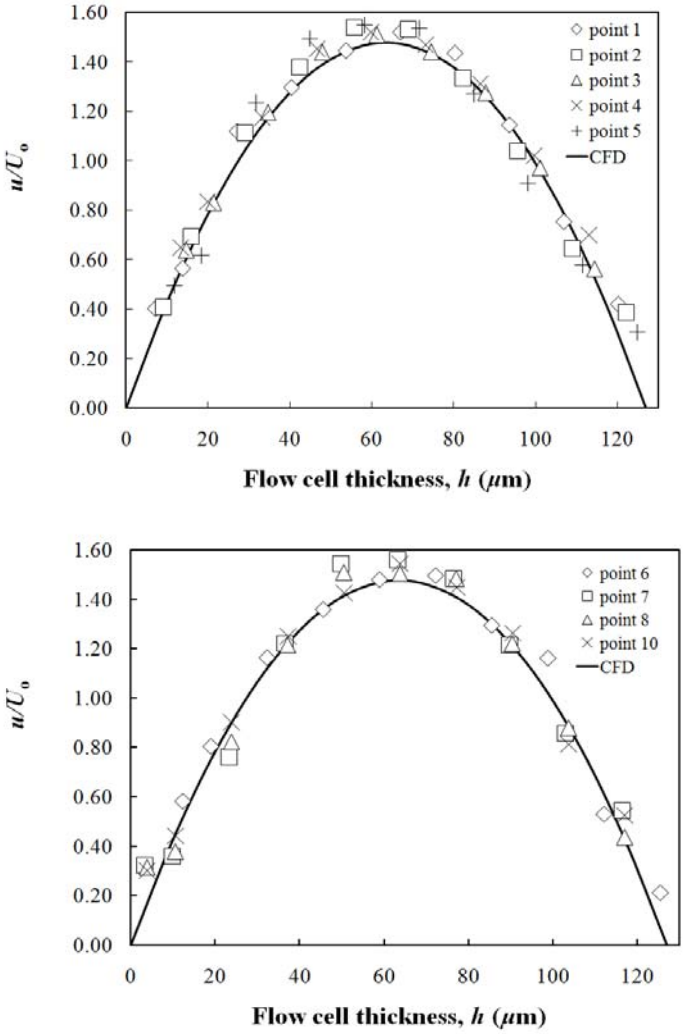

Figure 3 Velocity Profiles as Obtained by Micro-PIV for Q = 0.414 ml/min.

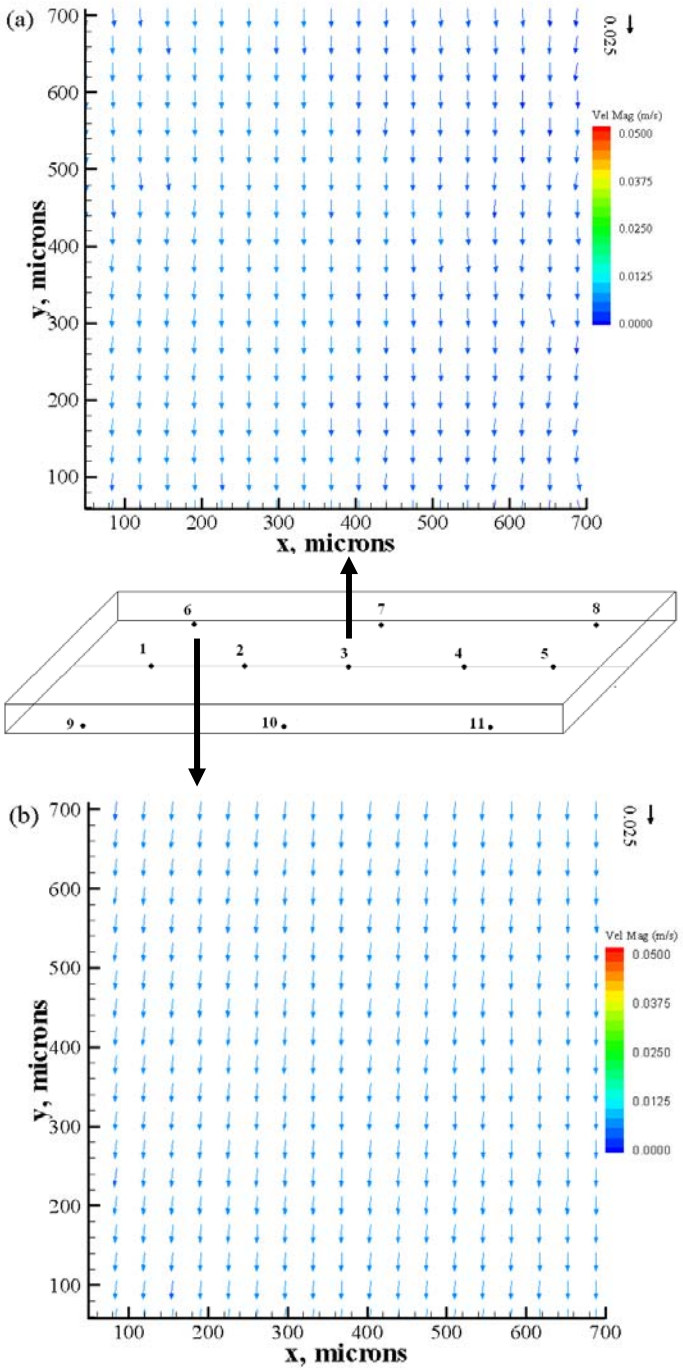

Figure 4 Velocity Field as Obtained by Micro-PIV (Without Endothelial Cells); (a) Point 3; (b) Point 6.

Due to the high aspect ratio of the flow chamber, the flow field is uniform for most of the measurement locations (Fig. 4), and the surfaces are exposed to the target stress level across the channel (Table 3). Points near the inlet and outlet ports (*e.g.* points 1 and 5 in Fig. 1*c*) also demonstrate insignificant variance in the wall shear stress values. The two-dimensionality of the channel is confirmed by Fig. 5 that shows uniformity of

wall shear stress profiles in span-wise directions for both target stresses. Thus, both micro-PIV measurements and CFD predictions show that the fluid velocity defining the local mechanical environment is location independent and the usage of this chamber in measuring specific cell response seems appropriate.

Point	(a) τ_w (dyn/cm^2)		(b) τ_w (dyn/cm^2)
	PIV	CFD	PIV
1	2.01	2.028	9.91
2	2.02	2.029	10.05
3	2.04	2.029	9.91
4	1.99	2.029	10.26
5	2.06	2.027	10.61
6	1.99	2.030	10.18
7	2.04	2.029	9.91
8	2.05	2.031	9.92
10	2.01	2.029	9.96

Table 3: Wall Shear Stress as Determined by Micro-PIV and CFD; (a) τ_{target} = 2 dyn/cm^2; (b) τ_{target} = 10 dyn/cm^2.

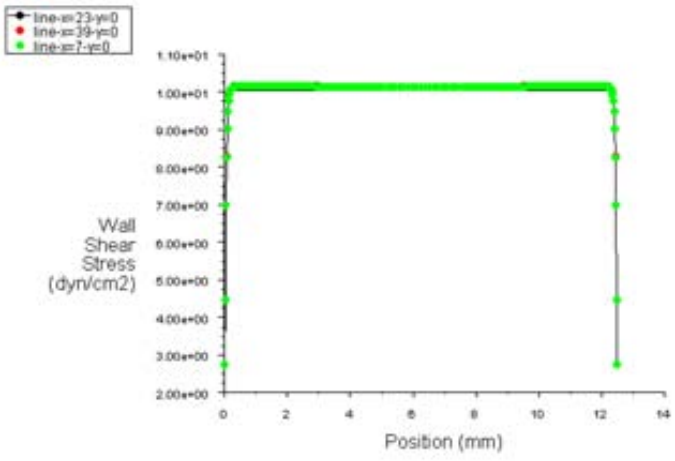

Figure 5 Wall Shear Stress Profiles Across the Chamber.

With Endothelial Cells

Once endothelial cells are introduced, local shear variations are large and the velocity profiles are no longer uniform. Due to the velocity differences between peaks and valleys, the local wall shear stresses range between 47-164% of the nominal values (*e.g.* without endothelium, target 2 dyn/cm^2, Table 4). The average thickness and standard deviation of the endothelial cells (including gelatine substrate) were 20.1 μm and 3.9 μm, respectively. The peaks to trough values compare extremely well with surface height variations of Voorhees et *al.* [12], 3.7 μm and Barbee et *al.* [14], 3.39 μm. This result challenges the basic assumption that all cells in a cells monolayer experience the desired target stress set using the idealized formula for calculating shear stress at the wall in a parallel plate model, which is the basic paradigm underlying most parallel plate flow chamber designs and their implementation. The computational model predictions match the experimental within the 3% experimental uncertainty.

The chamber flow area is reduced in the presence of endothelial cells (results in blockage increase). Flow acceleration occurs along streamlines toward the peaks by continuity. As a result, the wall shear stress is no longer constant within the area. Average velocity varies as a function of location (no longer uniform within the flow cell as shown in

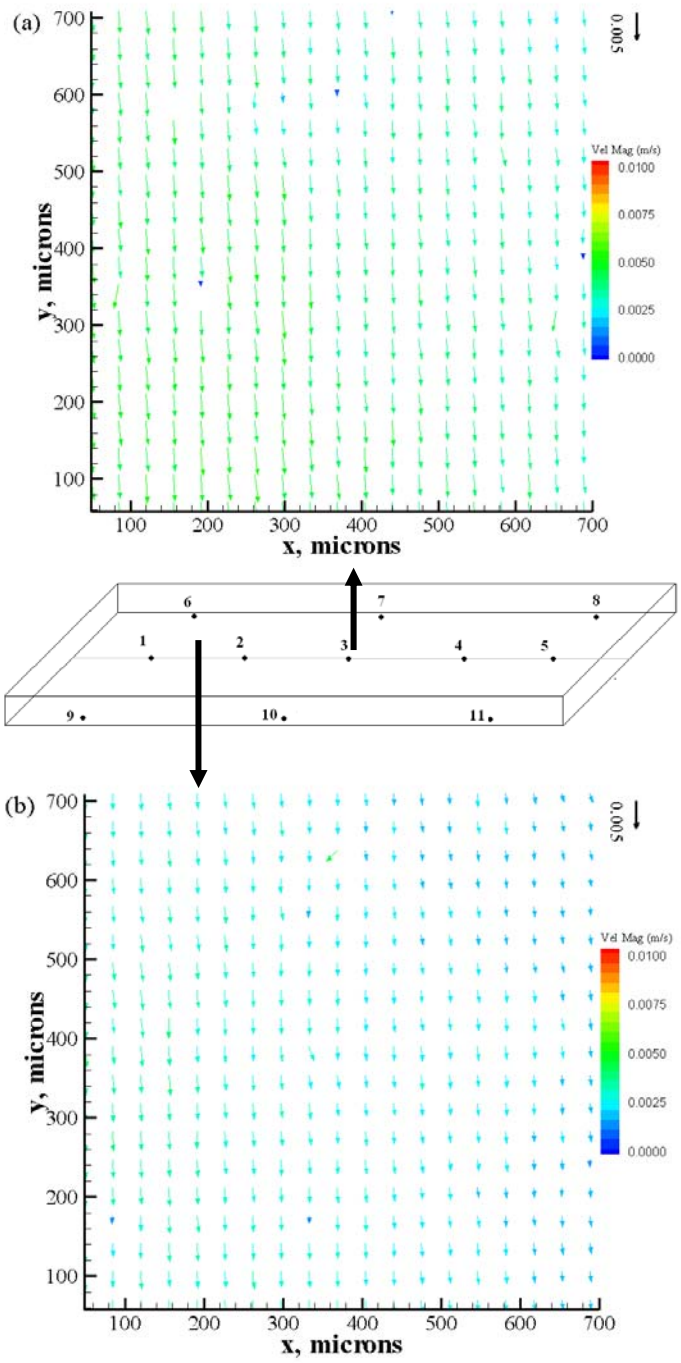

Figure 6 Velocity Field as Obtained by Micro-PIV (With Endothelial Cells); (a) Point 3; (b) Point 6.

Figs. 6 and 7). Since flow was steady and laminar, spatial variations in velocity can be assumed to be due to endothelial cells height variations. The average wall shear stress based on 9 PIV measurement locations is 4.21 dyn/cm^2 compared to 3.90 dyn/cm^2 area weighted average wall shear stress by CFD.

Point	Cell thickness (μm))	τ_w (dyn/cm^2)
1	21.9	3.83
3	26.2	4.67
5	17.3	3.77
6	14.8	3.64
7	22.8	5.27
8	17.3	5.27
9	23.6	3.89
10	24.6	4.62
11	18.3	2.93

Table 4 Wall Shear Stress as Determined by Micro-PIV.

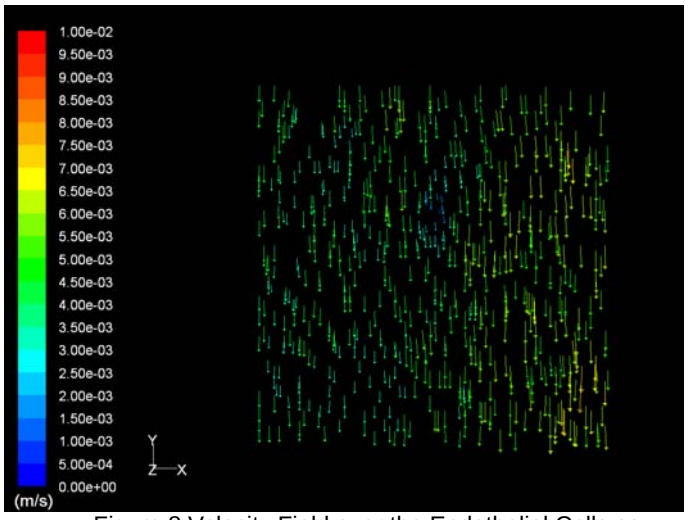

Figure 8 Velocity Field over the Endothelial Cells as Determined by CFD.

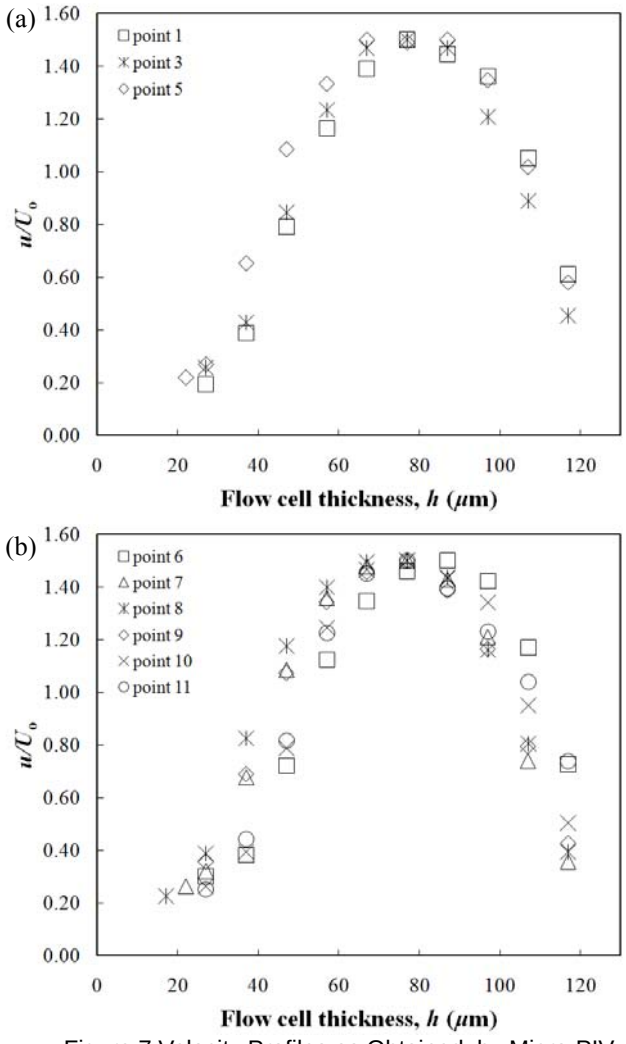

Figure 7 Velocity Profiles as Obtained by Micro-PIV; (a) Centerline; (b) Sides.

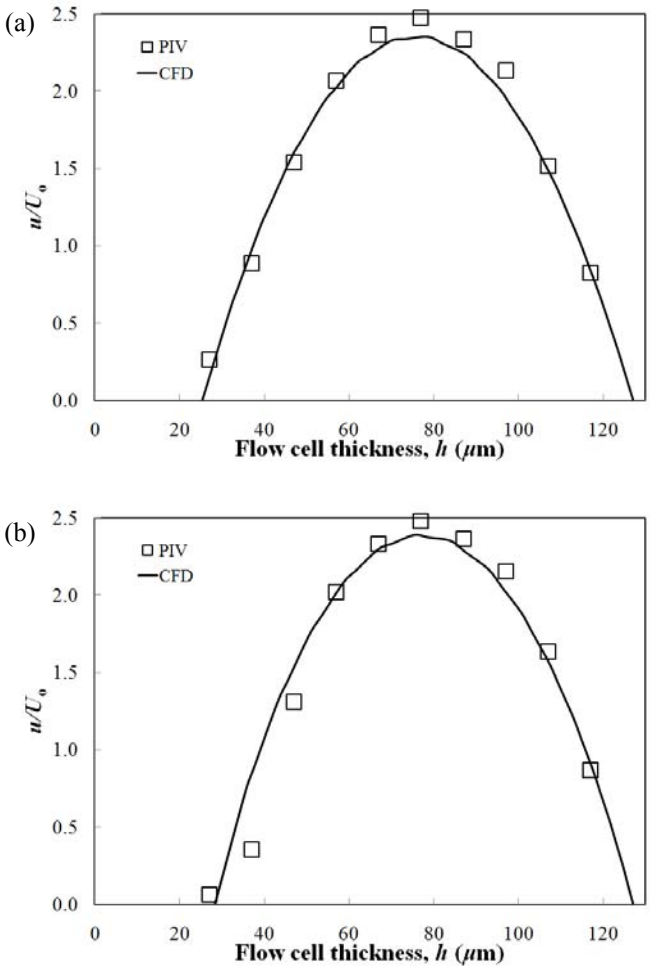

Figure 9 Velocity Profiles over the Cell as Obtained by Micro-PIV and CFD at Point 6;
(a) (x, y) = (100 μm, 150 μm); (b) (x, y) = (250 μm, 650 μm).

The cell monolayer topography (cell thickness) was mapped as described in the methodology section and the velocity fields were simulated (Fig. 8). Sample velocity distributions over the cells obtained by micro-PIV are compared with the numerical results and they are in good agreement (Fig. 9). Figure 10 shows the velocity field as obtained by micro-PIV superimposed on the image of underlying endothelial cells. The measurement plane was 35 μm from the lower wall. Dark spots can be interpreted as peaks of the cells. The velocity magnitude is lower at the peaks of the cells due to the fact that the measurement plane is closer to the cells, and higher in between cells (valleys) as shown in Fig 10. Again, the results are in good agreement with the simulation shown in Fig. 9.

The shear stress was correlated with the surface height and its distribution (by CFD) is shown in Fig 11. The results show that the distribution of shear stress depends on the shape and orientation of the cells. Higher shear stresses are found at the peaks; while the lower shear stresses are found at the valleys where the velocity vectors are weaker (as shown in Fig. 12). The findings are consistent with the numerics of [11, 14 and 15]. Non-uniform shear stress of significant magnitude across a cell surface could be of potential importance for explaining flow induced morphological changes [18, 19, 20]. Since we are proposing that the cells are sensitive to the subcellular distribution of shear stress, then the biological responses of individual cells ought to show the same variability. Endothelium exposed to large shear stress gradients display increased cell division, changes in cell density, altered growth factor and metabolism, surface adhesive properties and changes permeability to macromolecules [15].

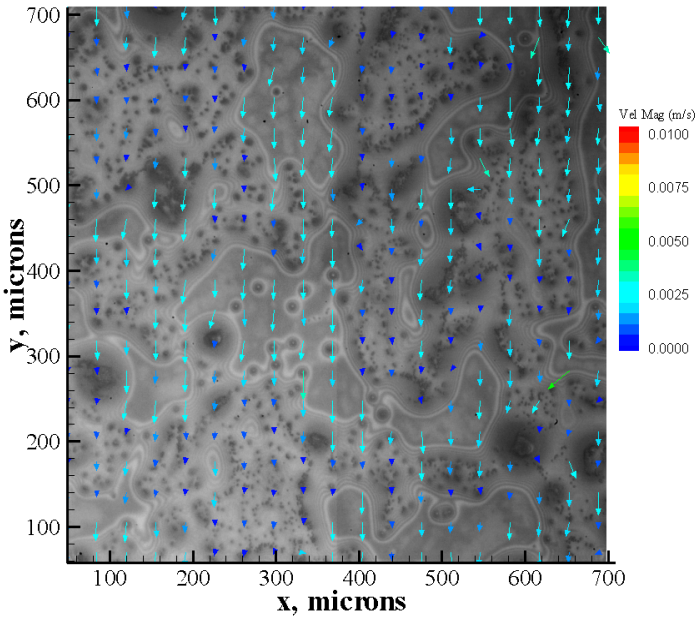

Figure 10 Velocity Field over the Endothelial Cells as Determined by Micro-PIV.

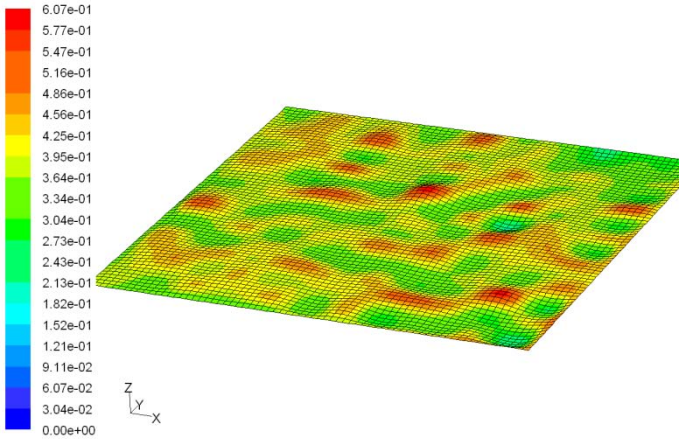

Figure 11 Wall Shear Stress Distribution over the Endothelial Cells as Determined by CFD (unit is in Pa).

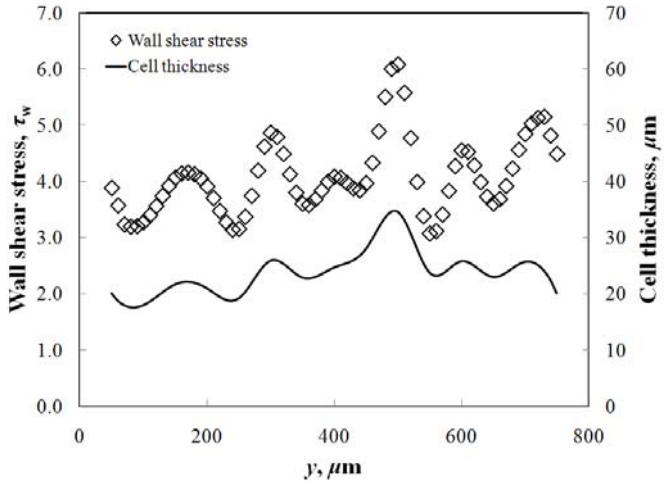

Figure 12 Wall Shear Stress Profiles along the Stream-wise Line at x = 400 μm. The Corresponding Cell Thickness is also shown.

CONCLUSION

Our parallel-plate flow chamber can be used to apply a well controlled flow regime to cultured cells (*e.g.* for cell adhesion and vascular infection studies). Without endothelial cells, the flow field is uniform over 95% of the chamber cross-section. This work also shows the capabilities of micro-PIV and CFD in obtaining the flow field over endothelial cells and the wall shear stress distribution over irregular cell surfaces. This study demonstrates that the non-uniform shear stress distribution over cells is non-negligible (*e.g.* significant in small vessels or where blockage is important). Study of the distribution of forces on cells aids in understanding the role of shear stress in the pathophysiology of atherosclerosis. This work lays the groundwork for future work involving endothelial cells in pulsatile flow in unsteady hydrodynamic conditions (*e.g.* backward-facing step).

ACKNOWLEDGEMENT

M. Mehdi Salek would like to acknowledge the Alberta Ingenuity, now part of Alberta Innovates Technology Futures, for his financial supports through a scholarship. Rinker and Martinuzzi acknowledge financial support through the NSERC Discovery program.

REFERENCES

[1] Malek, A. M., Alper, S. L., and Izumo, S., 1999, "Hemodynamic Shear Stress and its Role in Atherosclerosis," Journal of the American Medical Association, **282**, pp. 2035–2042.

[2] Tardy, Y., Resnick, N., Nagel, T., Gimbrone Jr., M. A., and Dewey Jr., C. F., 1997, "Shear Stress Gradients Remodel Endothelial Monolayers in Vitro via a Cell Proliferation-Migration-Loss Cycle," Arteriosclerosis, Thrombosis, and Vascular Biology, **17**, pp. 3102–3106.

[3] Traub, O., and Berk, B. C., 1998, "Laminar Shear Stress Mechanisms by Which Endothelial Cells Transduce an Atheroprotective Force," Arteriosclerosis, Thrombosis, and Vascular Biology, **18**, pp. 677-685.

[4] Klevens, R. M., Edwards, J. R., Tenover, F. C., McDonald, L. C., Horan, T., and Gaynes, R., 2006, "Changes in the Epidemiology of Methicillin-Resistant *Staphylococcus aureus* in Intensive Care Units in US Hospitals, 1992–2003," Clinical Infectious Diseases, **42**, pp. 389-391.

[5] Chung, B. J., Robertson, A. M., and Peters, D. G., 2003, "The Numerical Design of a Parallel Plate Flow Chamber for Investigation of Endothelial Cell Response to Shear Stress," Computers & Structures, **81**, pp. 535-546.

[6] Helmlinger, G., Geiger, R. V., Schreck, S., Nerem, R. M., 1991, "Effects of Pulsatile Flow on Cultured Vascular Endothelial Cell Morphology," Journal of Biomechanical Engineering, **113**, pp. 123-131.

[7] Dardik, A., Chen, L., Frattini, J., Asada, H., Aziz, F., Kudo, F. A., Sumpio, B. E., 2005, "Differential Effects of Orbital and Laminar Shear Stress on Endothelial Cells," Journal of Vascular Surgery, **41**, pp. 869-880.

[8] Ruel, J., Lemay, J., Dumas, G., Doillon, C., Charara, J., 1995, "Development of a Parallel Plate Flow Chamber for Studying Cell Behavior Under Pulsatile Flow," American Society for Artificial Internal Organs Journal, **41**, pp. 876-883.

[9] Anderson, E. J., Falls, T. D., Sorkin, A. M., and Tate, M. L. K., 2006, "The Imperative for Controlled Mechanical Stresses in Unraveling Cellular Mechanisms of Mechanotransduction," Biomedical Engineering Online, **5**, pp. 1-14.

[10] McCann, J. A., Peterson, S. D., Plesniak, M. W., Webster, T. J., and Haberstroh, K. M., 2005, "Non-Uniform Flow Behavior in a Parallel Plate Flow Chamber Alters Endothelial Cell Responses," Annals of Biomedical Engineering, **33**, pp. 328-336.

[11] Barbee, K. A., 2002, "Role of Subcellular Shear-Stress Distributions in Endothelial Cell Mechanotransduction," Annals of Biomedical Engineering, **30**, pp. 472–482.

[12] Voorhees, B. A., Nackman, G. B., and Wei, T., 2007, "Experiments Show Importance of Flow-Induced Pressure on Endothelial Cell Shape and Alignment," Proceedings of the Royal Society A, **463**, pp. 1409-1419.

[13] Barbee, K. A., Davies, P. F., and Lal, R., 1994, "Shear Stress-Induced Reorganization of the Surface-Topography of Living Endothelial-Cells Imaged by Atomic-Force Microscopy," Circulation Research, **74**, pp. 163–171.

[14] Barbee, K. A., Mundel, T., and Davies, P. F., 1995, "Subcellular Distribution of Shear Stress at the Surface of Flow-aligned and Nonaligned Endothelial Monolayers," Am J Physiol Heart Circ Physiol, **268,** pp. H1765-H1772.

[15] Satcher, R. L., Bussolari, S. R., Gimbrone, M. A., and Dewey, C. F., 1992, "The Distribution of Fluid Forces on Model Arterial Endothelium Using Computational Fluid-Dynamics," Journal of Biomechanical Engineering, Transactions of the ASME, **114**, pp. 309–316.

[16] Devasenathipathy, S., Santiago, J. G., Wereley, S. T., Meinhart, C. D., and Takehara, K., 2003, "Particle Imaging Techniques for Microfabricated Fluidic Systems," Experiments in Fluids, **34**, pp. 504-514.

[17] Meinhart, C. D., Wereley, S. T., and Gray, M. H. B., 2000, "Volume Illumination for Two-Dimensional Particle Image Velocimetry," Measurement, Science and Technology, **11**, pp. 809-814.

[18] Potter, D. R., and Damiano, E. R., 2008, "The Hydrodynamically Relevant Endothelial Cell Glycocalyx Observed In Vivo Is Absent In Vitro," Circulation Research, **102(7)**, pp. 770-776.

[19] McKinney, V. M., Rinker, K. D., and Truskey, G. A., 2006, "Normal and Shear Stresses Influence the Spatial Distribution of Intracellular Adhesion Molecule-1 Expression in Human Umbilical Vein Endothelial Cells Exposed to Sudden Expansion," Journal of Biomechanics, **39**, pp. 806-817.

[20] Shepherd, R. D., Kos, S. M., Rinker, K. D., 2009, "Long-term Pulsatile Shear Stress Leads to Increased Phosphorylation of Multiple MAPK Species in Cultured Human Aortic Endothelial Cells," Biorheology, **46:6**, pp. 529-538.